Northumbria
University
NEWCASTLE

Reduction-Responsive Amphiphilic Star Copolymers with Long-chain Hyperbranched Poly(ε-caprolactone) Core and Disulfide Bonds for Trigger Release of Anticancer Drugs

Shan Zhang[a], Yinglai Hou[a], Heng Chen[b], Zijun Liao[c], Jianxin Chen[a], Ben B. Xu[d]*, Jie Kong[a]*

[a]Shaanxi Key Laboratory of Macromolecular Science and Technology, School of Science, Northwestern Polytechnical University, Xi'an, 710072, P. R. China

[b]Shenzhen Key Laboratory of Special Functional Materials, College of Materials Science and Engineering, Shenzhen University, Shenzhen, 518060, P. R. China

[c]Department of Fundamentals, Army Logistics University of PLA, Chongqing, 401311, P. R. China

[d]Smart Materials and Surfaces Lab, Faculty of Engineering and Environment, Northumbria University, Newcastle upon Tyne, NE1 8st, UK

*Corresponding Authors

E-mail: kongjie@nwpu.edu.cn (J. K.); ben.xu@northumbria.ac.uk (B. X.).

Abstract: In this contribution, the reduction-responsive star copolymers with long-chain hyperbranched poly(ε-caprolactone) (PCL) (HyperMacs) core and disulfide bonds were synthesized *via* Cu(I)-catalyzed azide-alkyne cycloaddition (CuAAC) reaction. The HyperMacs core was constructed from disulfide-containing AB_2-type PCL macromonomers, which possesses length-adjustable chain segments between branching points, large cavities, low degree of crystallinity, and reduction-responsivity. After grafted with poly(ethylene glycol), the reduction-responsive star copolymers can self-assemble into micelles in aqueous solution. The obtained micelles exhibited much lower critical micelle concentration (CMC) than their linear analogues. The reduction-responsivity from disulfide bonds makes them a promising carrier candidate for trigger release of anticancer drugs. The *in vitro* release results confirmed that their doxorubicin (DOX)-loaded micelles exhibited desirable reduction-triggered release performance. The cellular proliferation inhibition against HepG2 cells demonstrated that the DOX-loaded micelles showed a comparable anticancer activity with free DOX. Therefore, it can be expected that the reduction-sensitive micelles may serve as smart vehicles for intracellular delivery of anti-cancer drugs in tumour therapy.

1. Introduction

Polymeric micelles self-assembled from amphiphilic copolymers have currently emerged as an important drug carrier because they enhance drug solubility, prolong blood circulation time and reduce toxic and side effect [1-3]. The traditional linear amphiphilic polymer micelles are prone to early leakage due to dilution effects of blood circulation before they reach lesion sites, reducing the drug efficiency [4]. Improving the stability of polymeric micelles has been an important issue in drug delivery. Cross-linking is an effective method to improve the stability of polymeric micelles, and various strategies have been used to prevent micelles disintegration and premature drug leakage when diluting in the bloodstream [5-7]. Normally, the micelle cores are constructed with hydrophobic biocompatible polymers to load hydrophobic drugs. Although various polymers have been utilized as hydrophobic cores of micelles, two important types hydrophobic polymers approved by United States Food and Drug Administration (FDA), i.e. poly lactic acid (PLA) and poly(ε-caprolactone) (PCL), receive much more attentions for their excellent biocompatibility and biodegradability [8,9]. However, cross-linking strategy is unsuitable for these linear polymers [10-12]. Furthermore, the crystallization of PCL is an intrinsic drawback that reduces drug loading content and further decreases drug loading efficiency of drug delivery system [13-15]. This problem significantly hampers the practical applications of PCL-based polymeric micelles.

Hyperbranched or highly branched polymers possess three-dimensional topological structure with large cavities, and their crystallization ability is limited by the branched structure [16-21]. Therefore, constructing hyperbranched hydrophobic core is a promising alternative to cross-linking strategy of PCL-based polymeric micelles. Normally, PCL is a linear polymer derived from *ε*-caprolactone through ring-opening polymerization, and it is intractable to directly prepare hyperbranched PCL from small monomer strategy [22-24]. Long-chain hyperbranched polymers (HyperMacs) are distinctive hyperbranched polymers that are typically prepared by polycondensation of AB_2-type macromonomers.[25-31] By tuning the molecular

weight of macromonomers, the chain length and looseness between branching points can be well adjusted.[32,33] Moreover, Compared to traditional hyperbranched polymers, they have larger topological cavity and are much more suitable for hydrophobic core of micelles [34]. Although HyperMacs type PCL has been prepared by Kwak and Gao et al. [23,35], the utilization of HyperMacs PCL to construct a star copolymer for polymeric micelle has never been reported and it deserves further investigation.

On the other hand, for enhancing delivery and therapy efficiency, it is necessary to release anticancer drugs in targeted sites. The stimuli-responsive micelles can retain the drugs in the blood circulation and release them under appropriate stimulus triggering, such as pH, light, temperature, magnetic and reductive environment [30-37]. Notably, reductive agent glutathione (GSH) has been regarded as a significant signal for distinguishing tumour tissue from normal tissue [38]. *In vivo* research has confirmed that tumour tissues showed much higher GSH concentration than that of normal tissues [45]. Disulfide, a reduction-responsive group without physiological toxicity, can be cleaved *via* the thiol-disulfide exchange reaction [39-42]. The specific structure of disulfide bond containing polymers exhibit ideal physicochemical properties in material science, tissue engineering and targeted gene or drug delivery [43-46]. The introduction of disulfide bond into HyperMacs PCL will bring reduction-responsivity and endow polymeric micelle new function of triggered release.

In this work, a disulfide bond-containing and “clickable” PCL-based AB2 macromonomer was designed to construct new reduction-responsive PCL HyperMacs via Cu(I)-catalyzed azide-alkyne cycloaddition (CuAAC) reaction. After grafted with poly(ethylene glycol) (PEG), amphiphilic and reduction-responsive star copolymers was obtained. The star copolymers can self-assemble into micelles in aqueous solution and serve as new drug-carrier for triggered release of anticancer drugs. Using DOX as model drug, the reduction-responsive release behaviour of the drug-loaded

micelles, the intracellular release of DOX, and the inhibition of cellular proliferation of HepG2 cells by DOX-loaded micelles was fully investigated.

2. Experimental Section

2.1. Materials

3-chloro-1, 2-propanediol (99%, Xiya Reagent), 3,3'-dithiobispropionic acid (99%, Aladdin), sodium azide (>99%,Amresco), propargyl alcohol (>99%, Xiya Reagent), 1-ethyl-3-(3-dimethylaminopropyl)-carbodiimide hydrochloride (EDC·HCl, 99%, J.&K. Chemical), 4-dimethylaminopyridine (DMAP, 99%, J.&K. Chemical), ε-caprolactone (99%, J.&K. Chemical), Tin(II) 2-ethylhexanoate ($Sn(Oct)_2$, 96%, Alfa Aesar Tianjing Co.), monomethoxy poly(ethylene glycol) (MPEG, M_w=5000 Da, Aladd Shanghai Co.), Hoechst 33258 (Beyotime Biotechnology, Jiangsu, China), Cell Counting Kit (CCK-8, Beyotime Biotechnology, Jiangsu, China), Azido-functionalized Merrifield resin was prepared according to a previously reported method [38].

2.2. Characterization

Fourier transform infrared spectroscopy (FT-IR) measurement was conducted using an FT-IR spectrophotometer (Perkin-Elmer, USA). Nuclear magnetic resonance (NMR) measurements were carried out on a Bruker Avance 500 spectrometer (Bruker BioSpin, Switzerland) operating at 50.7 MHz in $CDCl_3$ or $DMSO_6$. Chemical shifts are referenced to tetramethylsilane (TMS). Size exclusion chromatography (SEC) measurements were conducted using a system equipped with a Waters 515 pump, an autosampler, and two MZ gel columns (10^3 Å and 10^4 Å) with a flow rate of 0.5 mL min^{-1} in DMF (HPLC grade) at 25 °C. Detectors were including a differential refractometer (Optilabr EX, Wyatt) and a multi-angle light scattering detector (MALLS) equipped with a 632.8 nm He-Ne laser (DAWN EOS, Wyatt). The refractive index increment of polymers in DMF was measured at 25 °C using an Optilabr EX differential refractometer. ASTRA software (Version 5.1.3.0) was used for the acquisition and analysis of data. The morphologies of the micelles were observed by a transmission electron microscope (TEM, Hitachi-600, Japan). The

samples were prepared by directly dropping the solutions of micelles onto carbon-coated copper grids and allowed to dry at room temperature before measurement. The micelles size and size distribution (PDI) were measured using a laser particle size analyzer (Zetasizer Nano, Malvern, UK). Static light scattering (SLS) analysis was performed on a DAWN HELEOS-II multi-angle light scattering detector (Wyatt Technology Corporation, USA) operated at 665 nm, using gallium–arsenic as the incident laser beam source. SLS data were collected at 6 different concentrations of the aggregates and 18 different angles for each concentration. The average molecular weight values of the amphiphilic copolymers aggregate in aqueous solutions were obtained by the common Zimm method using HELEOS-II Firmware 2.4.0.4 advanced software. The melting temperature was measured with a Perkin-Elmer differential scanning calorimeter (DSC) at a heating and cooling rate of 10 K/min from -30 °C to 90 °C, under a nitrogen atmosphere. The crystallinity (X_C) of the PCL was calculated by the following formula:

$Xc=\Delta H_m/\Delta H_m^* \times 100\%$

where ΔH_m^* is 139 J/g, which is the theoretical heat of fusion for 100% crystalline PCL [47]. The cell uptake experiment was conducted by inverted fluorescence microscope (Olympus IX73). Cell viability was detected by M200 Pro Nano Quant (TECAN).

2.3. Preparation of clickable AB_2 macromonomer (M-AB_2-PCL)

The typical synthesis procedure is described as follows. Under an insert argon atmosphere, a 100 mL dry Schlenk flask was charged with 3-chloro-1,2-propanediol (0.22 g, 2 mmol), ε-caprolactone (4.56 g, 40 mmol) and $Sn(Oct)_2$ (13.0 μL, 0.04 mmol). The mixture was stirred for 24 h at 110 °C, then added with sodium azide (0.95 g, 15 mmol) and 60 mL DMF, and further stirred for another 36 h at 80 °C. After removing DMF by rotary evaporation, the residue was dissolved in ethyl acetate and passed through a short column of neutral alumina for the removal of sodium salts. After concentrated by rotary evaporation, azide functionalized AB_2-PCL was obtained as white solid. The obtained azide functionalized AB_2-PCL, MPDP (1.99 g, 8 mmol), EDC·HCl (1.91 g, 10 mmol) and DMAP (0.12 g, 1mmol) were added into 60 mL

dichloromethane. The mixture was stirred at room temperature for 24 h then the solvent was added with 100 mL DI water. The organic layer was collected, evaporated, and dried over anhydrous $MgSO_4$. After concentrated by rotary evaporation, the final product was precipitated twice into an excess cold diethyl ether and dried in vacuum oven (yield: 4.95 g, 73.1%). FT-IR (KBr, cm^{-1}): 3275 (s, -C≡C-H), 2106 (s, $-N_3$), 1740, 1710 (vs, C=O).^{1}H NMR ($CDCl_3$, ppm): 1.32-1.51 (-CO-CH_2-CH_2-C*H*$_2$-CH_2-CH_2O-), 1.51-1.82 (-CO-CH_2-C*H*$_2$-CH_2-C*H*$_2$-CH_2O-), 2.18-2.42 (-CO-C*H*$_2$-CH_2-CH_2-CH_2-CH_2O-), 2.51 (-CH_2-C≡C*H*), 2.80 (-C*H*$_2$-CH_2-SS-CH_2-C*H*$_2$-), 2.90 (-C*H*$_2$-SS-C*H*$_2$-), 3.58 (-C*H*$_2$-N_3), 4.21 (-C*H*$_2$-COO-CH_2-CH_2-CH_2-CH_2-CH_2O-), 4.74 (-C*H*$_2$-C≡CH), 5.25 (-C*H*-CH_2-N_3).

2.4. Synthesis of PCL-based HyperMacs (HB-PCL)

M-AB_2-PCL macromonomer (0.1 mmol) and $CuSO_4 \cdot 5H_2O$ (4.9 mg, 0.02 mmol) was dissolved in 2 mL DMF in a 10 mL flask, and then bubbled with nitrogen gas for 30 min, ascorbic acid (17.4 mg, 0.1mmol) was added quickly and the flask was immersed in an oil bath at 45 ^{o}C to initiate the polymerization. The reaction was allowed to react at room temperature for another 12 h. The reaction was quenched by diluted with 10 mL dichloromethane and exposed to air. And then, 3 equiv. of PMDETA ligand was added to exact out the Cu catalyst from the product. The obtained polymers were passed through an alumina column before being precipitated in ether (yield: 0.14 g, 56.1%). FT-IR (KBr, cm^{-1}): 2884 (vs, -CH_2-), 1740 (w, C=O). ^{1}H NMR ($CDCl_3$, ppm): 1.32-1.51 (-CO-CH_2-CH_2-C*H*$_2$-CH_2-CH_2O-), 1.51-1.82 (-CO-CH_2-C*H*$_2$-CH_2-C*H*$_2$-CH_2O-), 2.18-2.42 (-CO-C*H*$_2$-CH_2-CH_2-CH_2-CH_2O-), 2.51 (-CH_2-C≡C*H*), 2.80 (-C*H*$_2$-CH_2-SS-CH_2-C*H*$_2$-), 2.90 (-C*H*$_2$-SS-C*H*$_2$-), 3.50-3.52 (-C*H*$_2$-N_3), 4.21 (-C*H*$_2$-COO-CH_2-CH_2-CH_2-CH_2-CH_2O-), 4.68-4.81 (-C*H*$_2$-C≡CH, -SS-CH_2-CH_2-COO-CH_2-C*H*$_2$-triozle), 5.18-5.34 (triozle-C*H*$_2$-), 7.65-7.75 (triozle).

2.5. Synthesis of azido-functionalized methoxy poly(ethylene glycol) (azido mPEG)

p-Toluenesulfonyl chloride (3.81 g, 20 mmol) in pyridine (20 mL) was added in a 100 mL flask. The solution was cooled to 0 ^{o}C in ice-water bath before DMAP was added. Monomethoxypoly(ethylene glycol) (5.0 g, 1 mmol) in pyridine (20 mL) was added dropwise into the mixture under stirring. After stirring at ambient temperature for 12

h, the reaction mixture was diluted with 100 mL DI water and extracted with dichloromethane (3 times, 100 mL for each extraction). The combined organic solution was then washed with 100 mL 1 M HCl solution, and then washed with water (100 mL×3). The organic layer was rotary evaporated to dryness to give a white crystalline solid. The white solid was added into the mixture of sodium azide (3.9 g, 60 mmol) and 40 mL DMF. The mixture was stirred at 90 ^{o}C for 36 h and evaporated to remove DMF. The residue was dissolved in ethyl acetate and passed through a short column of neutral alumina for the removal of sodium salts. After concentrated by rotary evaporation, the residue was precipitated twice into an excess cold diethyl ether and dried in vacuum oven (Yield: 68%). FT-IR (KBr, cm^{-1}): 2102 (s, $-N_3$). ^{1}H NMR ($CDCl_3$, ppm): 3.38 (2H, (~O-CH_2-*CH_2*-N_3), 3.67 (broad, ~O-(*CH_2*-*CH_2*~)).

2.6. Preparation of star copolymers (SC-PCL-PEG)

HB-PCL (500 mg), azido-mPEG (0.15 g, 0.03 mmol), $CuSO_4{\cdot}5H_2O$ (7.48 mg, 0.03 mmol) and 3 mL DMF were mixed in a 10 mL flask. The mixture was degassed by three freeze-evacuate-thaw cycles followed by the addition of ascorbic acid (26.42 mg, 0.15 mmol) under the argon atmosphere and sealed. After stirring at 60 ^{o}C for 24 h, alkynyl-functionalized Merrifield resin was added and stirred for another 12 h. The polymer solution was diluted with dichloromethane and exposed to air to quench the reaction. 2 equiv. of PMDETA ligand was added to exact out the Cu catalyst. The obtained polymer in dichloromethane was then passed through an alumina column before being precipitated in diethyl ether. The final product was colorless with a yield around 60%. FT-IR (KBr, cm^{-1}): 2884 (vs, -CH_2-), 1740 (w, C=O). ^{1}H NMR ($CDCl_3$, ppm): 1.32-1.51 (-CO-CH_2-CH_2-C*H_2*-CH_2-CH_2O-), 1.51-1.82 (-CO-CH_2-C*H_2*-CH_2-C*H_2*-CH_2O-), 2.18-2.42 (-CO-C*H_2*-CH_2-CH_2-CH_2-CH_2O-), 2.51 (-C*H_2*-C≡CH), 2.80 (-C*H_2*-CH_2-SS-CH_2-C*H_2*-), 2.90 (-C*H_2*-SS-C*H_2*-), 3.50 (-C*H_2*-N_3), 3.59-3.88 (-O-C*H_2*-C*H_2*-O-, -O-C*H_2*-CH_2-triozle), 4.21 (-C*H_2*-COO-CH_2-CH_2-CH_2-CH_2-CH_2O-), 4.68-4.81 (-C*H_2*-C≡CH, -SS-CH_2-CH_2-COO-CH_2-C*H_2*-triozle), 5.18-5.34 (triozle-C*H_2*-), 7.65-7.75 (triozle).

2.7. Preparation of DOX-loaded micelles

The anticancer drug doxorubicin (DOX) was used as a model because of its

fluorescence properties. To obtain a high amount of DOX incorporation, triethylamine was added to remove hydrochloride from DOX·HCl. DOX-loaded micelles were prepared by a dialysis method as follows. Briefly, SC-PCL-PEG (25 mg) and DOX (8 mg) were dissolved in DMF (4 mL) under stirring 2 h, and then10 mL DI water was added dropwise to the mixture and stirred for another 2 h. The organic solvent was removed by dialysis against deionized water for 24 h (MWCO=50,000 g/mol), during which the water was renewed every 4 h and the whole procedure was performed in a dark room. To determine the total drug loading, the DOX-loaded micelle solution was lyophilized and then dissolved in DMF. The UV absorbance at 498 nm was measured to determine the DOX concentration. The drug loading content DLC (%) and drug loading efficiency DLE (%) were calculated based on the following equations:

DLC (%) = (weight of loaded drug/weight of polymer) × 100%

DLE (%) = (weight of loaded drug/weight of drug in feed) × 100%

2.8. In vitro reduction-triggered drug release

The DOX release from drug-loaded micelles (SC-PCL_{20}-PEG) was investigated at 37 °C in a phosphate-buffered saline (PBS) buffer solution (pH 7.4). Typically, the as-prepared DOX-loaded micelle solution was first suspended in 3 mL PBS or PBS with 0.1 mM of DTT and transferred into a dialysis membrane bag (MWCO=3,500 g/mol). The release experiment was initiated by immersing the end-sealed dialysis bag into 50 mL of the corresponding buffer solution in a shaking water bath at 37 °C in dark. At predetermined intervals, 3 mL of the release medium was taken out and replaced with an equal volume of fresh release medium. UV measurement was carried out to determine the content of the released DOX. All the results are expressed as the average data with standard deviations.

2.9. Cellular uptake of drug loaded micelles

HepG2 cells were seeded in 6-well plates at 1×10^5 cells per well in 1 mL complete Dulbecco's Modified Eagle Medium (DMEM), containing 10% fetal bovine serum (FBS) and supplemented with 1% penicillin/streptomycin, and cultured in a humid environment with 5% (*V*/*V*) CO_2 and 95% air at 37 °C for 24 h. After incubation for 24 h, the cells were washed with PBS and incubated for an additional 3 h with

DOX-loaded micelles (SC-PCL_{20}-PEG) at a final DOX concentration of 10 μg mL^{-1} in DMEM. Cells treated with free DOX were used as control. Then, the medium was removed, and the cells were washed three times with PBS. The cells were fixed with 4% formaldehyde for 30 min at room temperature, and the cells were washed three times with PBS. Finally, the cells were stained with Hoechst 33258 for 10 min. After replacement with PBS, the fluorescence images were obtained by using fluorescence microscope (Olympus, Japan).

2.10. In vitro cytotoxicity

HepG2 cells were seeded in 96-well plates at 1×10^4 cells per well in 100 μL of complete DMEM and incubated at 37 °C for 24 h. Then, the culture medium was removed and replaced with100 μL medium containing various concentrations of micelles from 25 to 1000 μg mL^{-1}, free DOX and DOX-loaded micelles (SC-PCL_{20}-PEG) with final DOX concentrations of 0.05 to 10 μg mL^{-1}. The untreated cells were used as the control. After further incubation of 24 h, the cells were incubated with fresh medium and CCK-8 solution at 37 °C for 4 h. And then quantified by an Infinite F200 (Tecan Inc., Switzerland) at a wavelength of 490 nm.

3. Results and Discussion

3.1. Synthesis and characterization of star copolymers

The synthetic route of star copolymers was shown in Scheme 1. First, 3-chloro-1, 2-propanediol initiated the ring-opening polymerization (ROP) of ε-caprolactone to generate AB_2-type PCL under the catalysis of $Sn(Oct)_2$. The primary and secondary hydroxyl groups of the initiator have different reactivities that may result to unequal chain length of AB_2 macromonomers theoretically. However, it has been reported that the ring-opening polymerization of ε-caprolactone was companied with intense transesterification,[48-49] and this transesterification would equilibrate the difference of macromonomer chain length caused by the reactivities of primary and secondary hydroxyl groups. Therefore, the difference of chain length of AB_2 macromonomers is neglected in this work. The AB_2-type PCL was further azidized with sodium azide, followed by esterification with MPDP, and azide- and alkyne-functionalized AB_2-PCL

macromonomer with disulfide bond was synthesized. The clickable AB_2-PCL macromonomer was named as M-AB_2-PCL_x where x refers to theoretical feed ratio of ε-caprolactone to 3-chloro-1, 2-propanediol. Then, $CuSO_4 \cdot 5H_2O$/ascorbic acid was employed to catalyze CuAAC click polymerization of M-AB_2-PCL_x, and a PCL-based HyperMacs (HB-PCL_x) was yielded. The HB-PCL_x was further grafted with azido-mPEG through CuAAC reaction, and star copolymer with PCL-based HyperMacs core and PEG shell (SC-PCLx-PEG) was obtained.

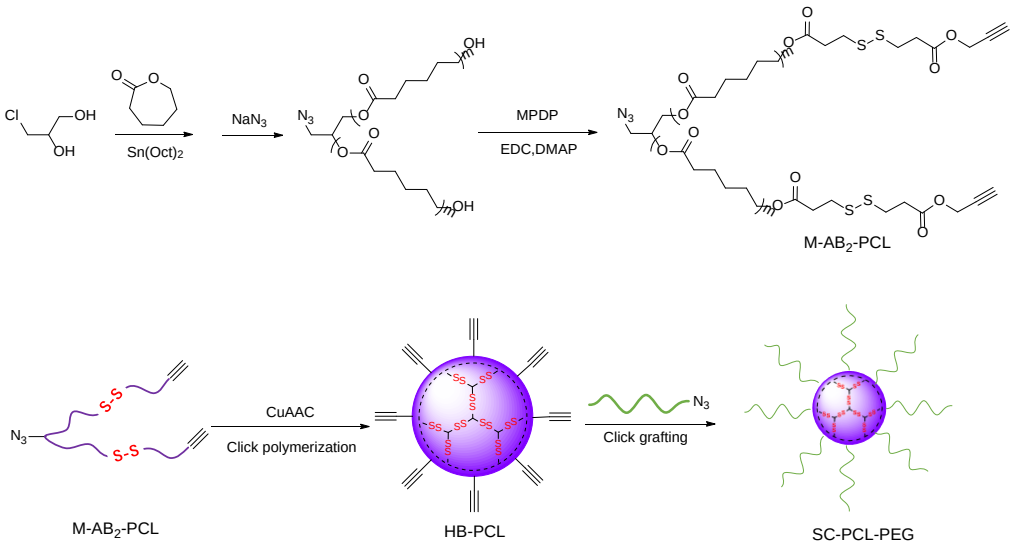

Scheme 1 The synthetic route of disulfide bonds containing star copolymers with HyperMacs core using ring-opening polymerization and CuAAC reaction.

These polymers were characterized by ^{1}H NMR, FTIR, and GPC. The ^{1}HNMR spectra of M-AB_2-PCL_{20}, HB-PCL_{20}, and SC-PCL_{20}-PEG were shown in Fig. 1 and characteristic signals of different protons were assigned with green labels. The signals at 3.58 and 4.74 ppm in the ^{1}H NMR spectrum of M-AB_2-PCL_{20} (Fig. 1a) were attributed to protons on methylene groups neighbored to azide and alkyne groups, respectively. The integration ratio of the two signals was calculated as 1: 2.08, and this result was consistent with their theoretical ratio of 1:2, suggesting that AB_2-type monomers have been synthesized. After click polymerization, the proton signals of methylene groups neighbored to alkyne groups decreased largely, and that neighbored to azide groups almost disappeared in the ^{1}HNMR spectrum of HB-PCL_{20} (Fig. 1b),

meanwhile, some new signals appeared at about 7.65-7.75 ppm suggested triazole units generated. After further click grafting, the proton signals of methylene groups neighbored to alkyne groups almost disappeared, and strong characteristic signals of the repeating PEO units appeared at 3.67 ppm in the ^{1}HNMR spectrum of SC-PCL$_{20}$-PEG (Fig. 1c). These changes revealed click polymerization and click grafting were well proceeded. Furthermore, in the FTIR spectra (Fig. 2a), M-AB$_2$-PCL$_{20}$ exhibited a strong peak of azide groups at 2106 cm^{-1} and a weak peak of alkyne groups 3275 cm^{-1}, and these peaks decreased greatly after click polymerization, and disappeared completely after click grafting. Moreover, GPC result also revealed the molecular weight of polymers increased gradually (Fig. 2b and Table 1). Note that the molecular weight of HyperMacs decreased with increasing molecular weight of AB$_2$ macromonomers. This phenomenon should be related to the long chains of AB$_2$ macromonomers that entangled together, wrapped azide and alkyne groups, and hindered the encounter between intermolecular azide and alkyne groups. In other words, the long chains of AB$_2$ macromonomers reduced the reactivities of azide and alkyne groups. In addition, the XPS spectrum (Fig. S1) showed that the SC-PCL$_{20}$-PEG was composed of carbon, oxygen, nitrogen, and sulfur elements, indicating the successful introduction of disulfide bonds into the star copolymers and complete removal of copper ions. These results demonstrated that M-AB$_2$-PCL$_x$, HB-PCL$_x$, and SC-PCL$_x$-PEG have been prepared successfully.

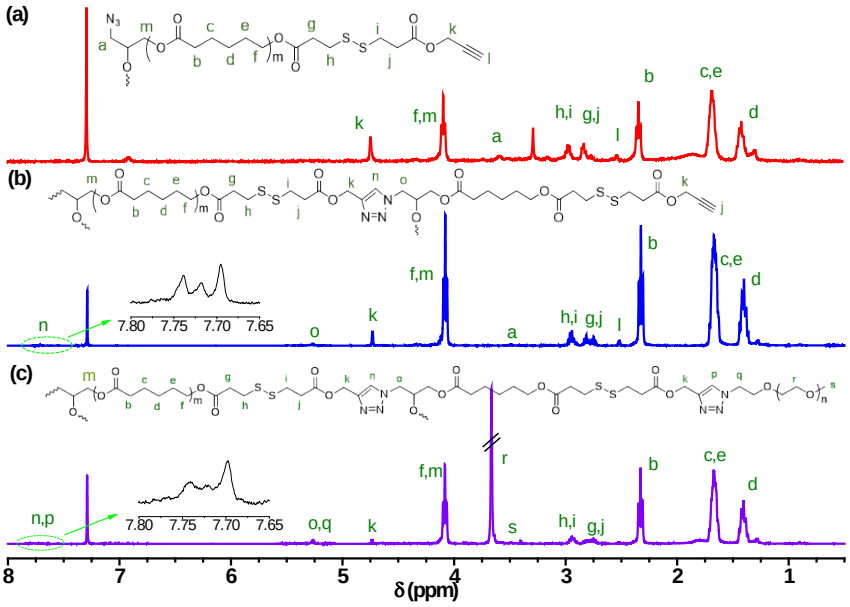

Fig. 1. ^{1}H NMR spectra of M-AB$_2$-PCL$_{20}$ macromonomer (a), HB-PCL$_{20}$ (b) and SC-PCL$_{20}$-PEG (c).

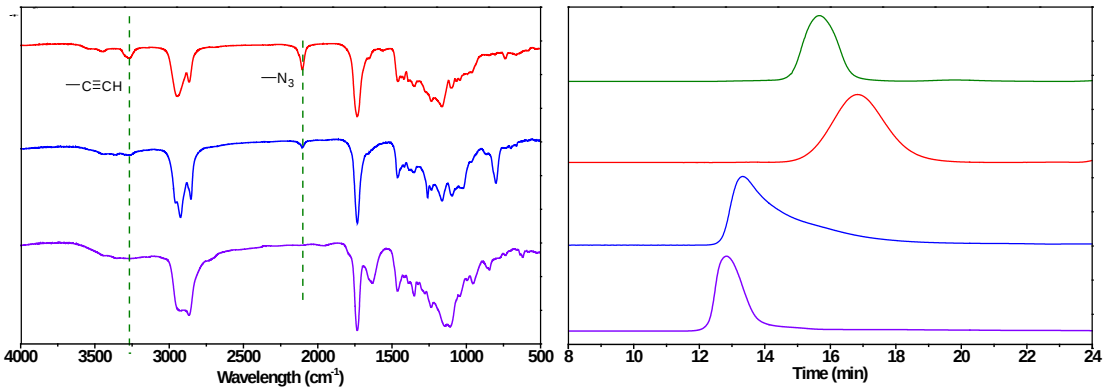

Fig. 2. (a) FT-IR spectra of M-AB$_2$-PCL$_{20}$ macromonomer (red curve), HB-PCL$_{20}$ (blue curve), and SC-PCL$_{20}$-PEG (purple curve); (b) SEC curves of azide-PEG (green), M-AB$_2$-PCL$_{20}$ macromonomer (red), HB-PCL$_{20}$ (blue), and SC-PCL$_{20}$PEG (purple).

Table 1

Molecular weight and molecular weight distribution of monomers, HyperMacs, and star copolymers.

Monomers	M_n[a]	M_n[b]	PDI[b]	HyperMacs	M_n[b]	PDI[b]	Star copolymers	M_n[b]	PDI[b]
M-AB$_2$-PCL$_{20}$	2 850	3 100	1.26	HB-PCL$_{20}$	69 000	1.25	SC-PCL$_{20}$-PEG	166 000	1.23

M-AB$_2$-PCL$_{30}$	3 990	4 200	1.21	HB-PCL$_{30}$	49 300	1.36	SC-PCL$_{30}$-PEG	85 400	1.32
M-AB$_2$-PCL$_{40}$	5 130	6 100	1.18	HB-PCL$_{40}$	41 900	1.28	SC-PCL$_{40}$-PEG	80 200	1.26

[a]Molecular weight was calculated theoretically based on feed ratio of 3-chloro-1,2-propanediol and ε-caprolactone. [b]Molecular weight and polydispersity index (PDI) were measured by GPC.

The crystallization of PCL has certain implications on the properties of PCL-based polymeric micelles, and typically higher PCL crystallinity will decrease its DLC [16]. Herein, the melting and crystallization behaviors of HyperMacs were investigated by DSC, and a linear PCL, L-PCL$_{20}$ (N_3-PCLm-SS-PCLm-N_3), was prepared for a comparison. The DSC thermograms of L-PCL$_{20}$ and HB-PCL$_{20}$ are shown in Fig. 3. Both melting temperature (41.3 ^oC) and crystallinity of HB-PCL$_{20}$ (38.7%) were lower than that of L-PCL$_{20}$ (50.8 ^oC and 66.3%, respectively). This phenomenon was mainly because that branched structures hindered regular arrangement of PCL segments and limited their crystallization, and this result suggested HyperbMacs strategy is an effectively way to reduce crystallization of PCL.

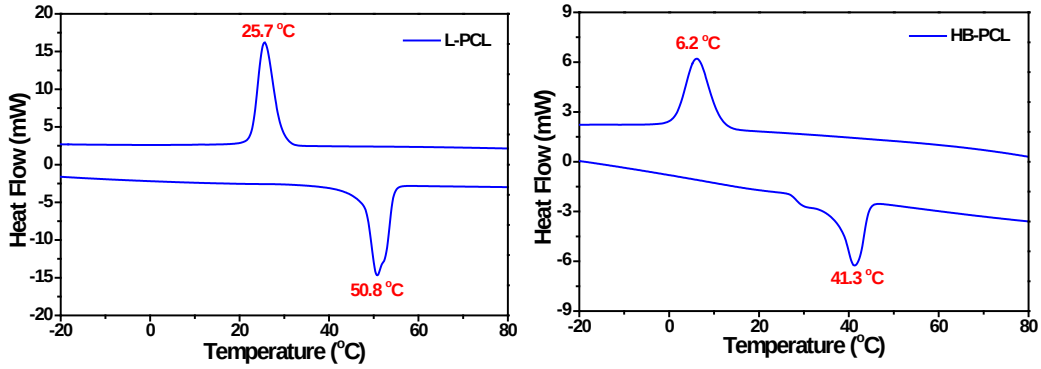

Fig. 3. DSC thermograms of L-PCL$_{20}$ (a) and HB-PCL$_{20}$ (b).

3.2. *Self-assembly in aqueous solution*

In this study, all original aggregates of amphiphilic copolymers were prepared in aqueous solution *via* dialysis method. The aggregates of these star copolymers are denoted as SC20 (SC-PCL$_{20}$-PEG), SC30 (SC-PCL$_{30}$-PEG), and SC40 (SC-PCL$_{40}$-PEG), respectively. Meanwhile, micelles of their linear counterparts were also prepared and denoted as LC20 (LC-PCL$_{20}$-PEG), LC30 (LC-PCL$_{30}$-PEG), and

LC40 (LC-PCL$_{40}$-PEG), respectively. The size and morphology of polymeric micelles have important influences on their *in vivo* performance, and they were investigated first by DLS and TEM. TEM images of polymeric micelles were shown in Fig. 4a-c, and it revealed that these star polymers formed stable spherical micelles in aqueous solution. Meanwhile, DLS results suggested these polymeric micelles exhibited monomodal distribution with hydrodynamic diameters around 60-80 nm (Fig. 4d-f). The particle size measured by DLS was larger than that by TEM, due to the swelling of the hydrophilic PEG shells in aqueous solution. Furthermore, SLS technique was used to analyze the averaged aggregation number of polymeric micelles (Table 2), and the averaged aggregation numbers of SC20, SC30, and SC40 were 6.0, 9.2, and 8.4, respectively. Compared to that of linear copolymers, the averaged aggregation numbers of these star copolymer micelles are much smaller, and this suggests these star copolymers are more prone to form stable micelles in aqueous solution. These micellar sizes form star copolymers are smaller than 200 nm allows them extravasate and accumulate in tumors via enhanced permeability and retention effect [51], and these micelles will be suitable for anticancer drug delivery applications.

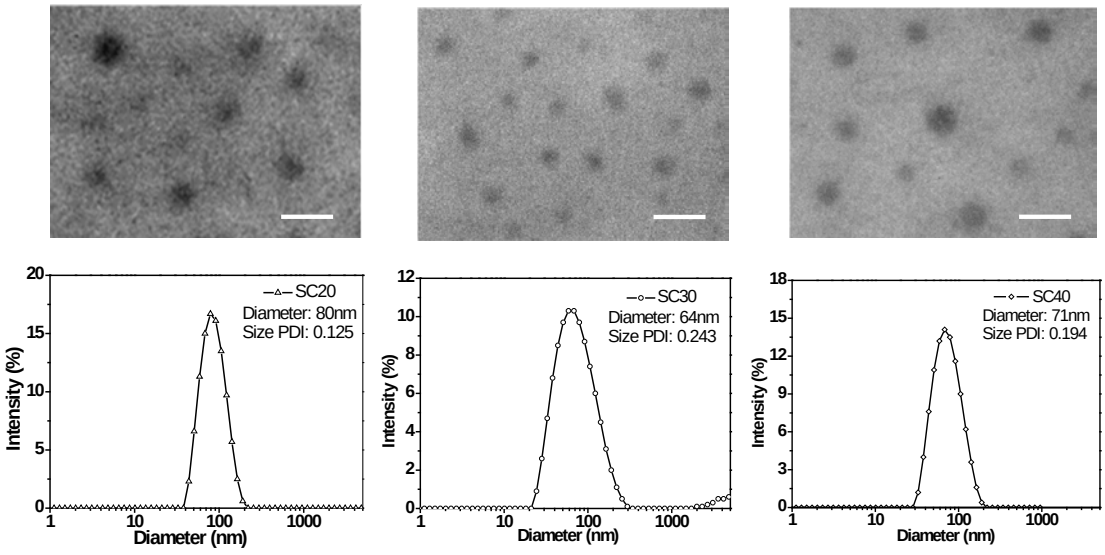

Fig. 4. TEM images of SC20 (a), SC30 (b), and SC40 (c), and DLS plots of SC20 (d), SC30 (e), and SC40 (f).

Critical micelle concentration (CMC) is the direct evidence of micellization, and it is

a key parameter to evaluate the stability of polymeric micelles. The CMC values of copolymers were determined by the fluorescence probe method using pyrene as a hydrophobic probe and carried out according to a reported method [52]. The CMC values of SC20, SC30, and SC40 at pH 7.4 were 0.69, 0.56, and 0.21 mg/ L (Fig. S2), respectively. In comparison, the CMC values of these star copolymers was almost one order of magnitude lower than that of linear counterparts (Table 2). These results confirmed that polymeric micelles from these star copolymers had higher stability than that of linear counterparts. The main reason probably is that these star copolymers have intrinsic core-shell structures, and these hyperbranched core structures play a role of discrete crosslink domains that effective reduce the risk of micellar disassembly. Furthermore, the drug loading capacity of polymeric micelles is also investigated. DOX was used as model of hydrophobic anti-cancer drug to be encapsulated into the polymeric micelles, and the results of DLC and DLE of polymeric micelles were listed in the Table 2. Obviously, polymeric micelles of star polymers exhibited much higher DLC and DLE than that of their linear counterparts. As analyzed above, these star polymers have HyperMacs core that has lower degree of crystallinity of PCL. Combining with their large cavities, these unique HyperMacs core contributes to load more hydrophobic drug moles in aqueous solution.

Table 2

Characterization data of star copolymers (SC-PCL-PEG) and properties of corresponding self-assembled micelles.

Samples	Diameter (nm)[a]	PDI[a]	$M_{w,agg}$ (g/mol)[b]	N_{agg}[c]	CMC (mg/L)	DLC (%)	DLE (%)
SC20	80	0.125	9.93×10^5	6.0	0.69	10.6	42.3
SC30	71	0.243	7.85×10^5	9.2	0.56	8.3	33.2
SC40	64	0.194	6.70×10^5	8.4	0.21	11.1	45.6
LC20	123	0.343	1.53×10^6	209.0	4.47	1.3	5.2
LC30	119	0.286	1.46×10^6	173.9	6.31	1.6	6.4
LC40	141	0.198	1.80×10^6	187.8	7.59	2.4	9.6

[a]Diameter and PDI of polymeric micelles were measured by DLS; [b]The weight-average molecular weight of polymeric aggregates in aqueous solution; [c]Average aggregation number (N_{agg}) was calculated by the ratio between $M_{w,\ agg}$ and

weight-average molecular weight of copolymers.

3.3. *Reduction-responsivity and in vitro drug release of polymeric micelles*

The HyperMacs core of star copolymers contained disulfide bonds, and this endowed star copolymers and their polymeric micelles reduction-responsivity. In this study, the reduction-responsive of polymeric micelles was evaluated with the reductant of DTT and the size change of micelles was monitored by DLS. The micelles were dispersed in PBS (pH 7.4) with 10 mM DTT, and a control group with 0 mM DTT. The size change of micelles in 48 h was illustrated in Fig. 5a. The size of micelles increased gradually over time in PBS with 10 mM DTT, while that in the control group remain stable in the 48 h. This indicated the micelles dissociated under the reductive environment. The dissociation of micelles was attributed the cleavage of disulfide groups that suffered from thiol/disulfide exchange with DTT [53].

The results confirmed the as-prepared micelles from disulfide bonds-containing star copolymers possessed good stability under physiological condition and reduction-cleavable property under reductive environment. Furthermore, *in vitro* DOX release behaviors of micelles were investigated in PBS with different DTT concentrations. The *in vitro* release profiles of DOX from micelles were shown in Fig. 5b. Obviously, the micelles exhibited a much faster release behavior of DOX in PBS with 10 m DTT than that in PBS without DTT. In detail, about 53% of the loaded DOX was released in PBS with DTT in the first 6 h, but only 13.4% was released in PBS without DTT. Over the whole 48 h test, more than 83% of the loaded DOX was released in PBS with DTT. In contrast, less than 25% was released in PBS without DTT. The in vitro drug release profiles clearly revealed that reductive environment accelerated the release of DOX from micelles of disulfide bond-containing star copolymers. These results confirm that these micelles had reduction-responsive drug release behavior, and this allows them suitable for triggered release of anticancer drug.

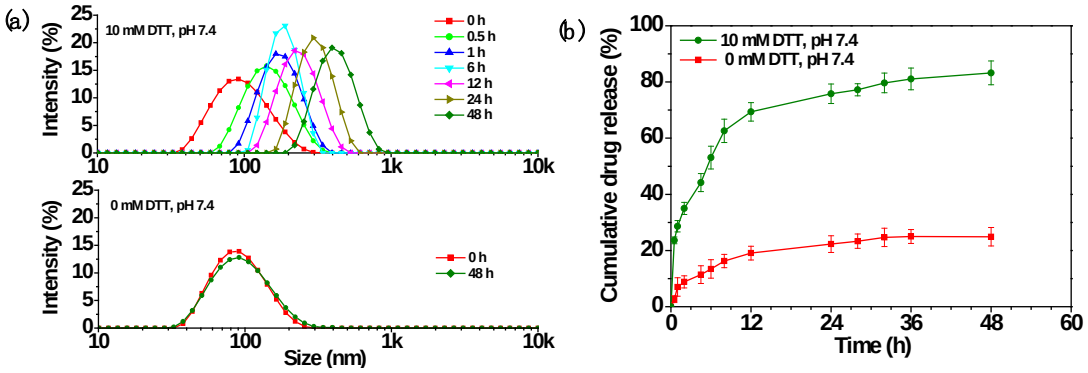

Fig. 5. (a) The size changes of SC20 micelles in PBS (pH 7.4), (b) *In vitro* DOX release from DOX-loaded micelles in PBS (pH 7.4).

3.4. Cellular uptake of drug-loaded micelles

The cellular uptake of DOX and DOX-loaded micelles was studied by fluorescence microscope using HepG2 cells. The red fluorescence from DOX and blue fluorescence from cell nucleus stained with Hoechst were used to monitor the intracellular localization of DOX within the cells [54]. Merged images displayed the overlay of red fluorescence of DOX and blue fluorescence of Hoechst staining of nuclei. In Fig. 6a, the cells exposed to free DOX for 1 h showed an obvious fluorescence signal in the nucleus and minimal fluorescence signal in cytoplasm (evidenced by red dots of DOX signal). In comparison with the blue fluorescence of the stained nucleus, HepG2 cells incubated with DOX-loaded micelles for 1 h displayed red fluorescence (Fig. 6b), indicating the efficient internalization of DOX-loaded micelles, GSH-triggered dissociation of micelles, and the release of DOX inside cells (as illustrated in Fig. 6e), and the longer incubation time (3 h) resulted in stronger DOX fluorescence in the nuclei of HepG2 cells in Fig. 6d. In contrast, the intracellular trafficking of DOX was significantly different for the cells incubated with free DOX. As shown in Fig. 6c, a relatively weak DOX fluorescence was observed in HepG2 cells after being cultured with free DOX for 3 h. The phenomenon was attributed to the fact that DOX-loaded micelles could be more efficiently internalized in HepG2 cells.

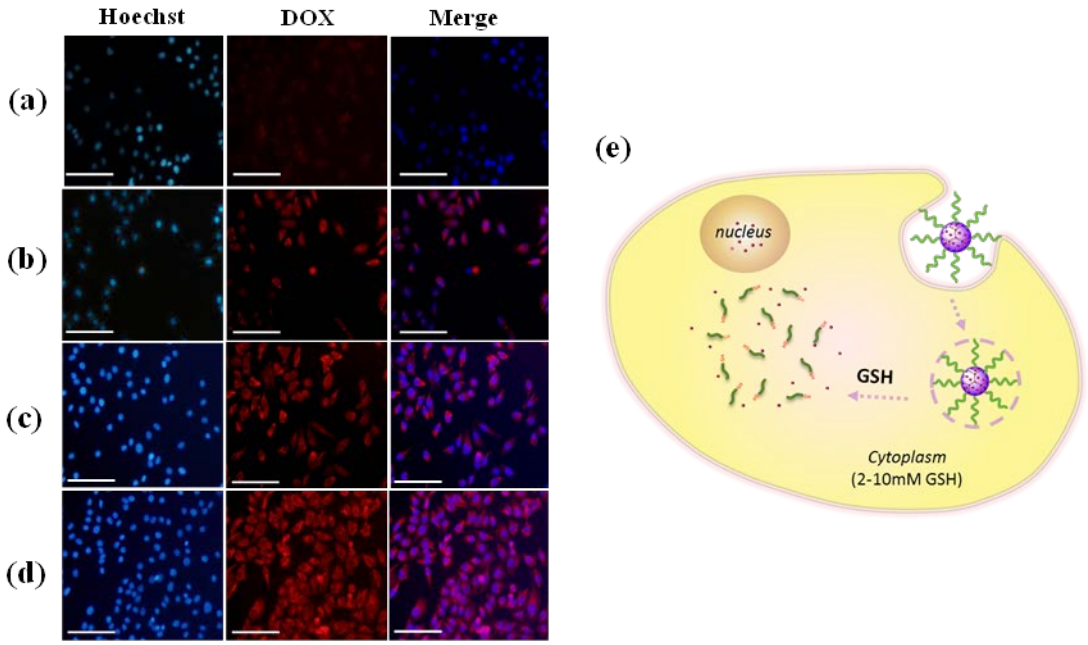

Fig. 6. Inverted fluorescence micrographs of HepG2 cells (scale bar 100 μm): cells were incubated with free DOX for 1 h (a), cells were incubated with DOX-loaded micelles for 1 h (b), cells were incubated with free DOX for 3 h (c), and cells were incubated with DOX-loaded micelles for 3 h (d), and schematic illustration of *in vitro* release of DOX-loaded SC micelles.

3.5. *In vitro cytotoxicity of polymeric micelles and antitumor activity of DOX-loaded micelles*

The *in vitro* cytotoxicity of polymeric micelles and the viability of HeLa cell treated with free DOX and DOX-loaded micelles (SC20) were evaluated *in vitro* using the Cell Counting Kit (CCK-8) assay. As shown in Fig. 7, with micelles concentrations up to 1000 μg/mL, cell viabilities were still higher than 90% after 24 h of incubation. Therefore, it can be considered that the micelles have no toxicity on HepG2 cells, and this indicates the micelles can be used as a good biocompatible carrier for drug delivery. After 24 h incubation, the DOX-loaded micelles showed comparable inhibition of HepG2 cells in comparison with free DOX (Fig. 7b), and this suggested DOX maintained its biological activity after incorporation into copolymer micelles. Moreover, as DOX concentration increasing, the DOX-loaded micelles showed increased cytotoxicity against HepG2 cells, more than 50% and 80% of HepG2 cells

died at an equivalent DOX concentration of 1 and 5μg/mL, respectively. Given instability of free DOX in blood circulation and the reduction-responsivity of the prepared micelles, it is concluded that the DOX-loaded micelles is a better choice for intracellular drug delivery systems for cancer chemotherapy.

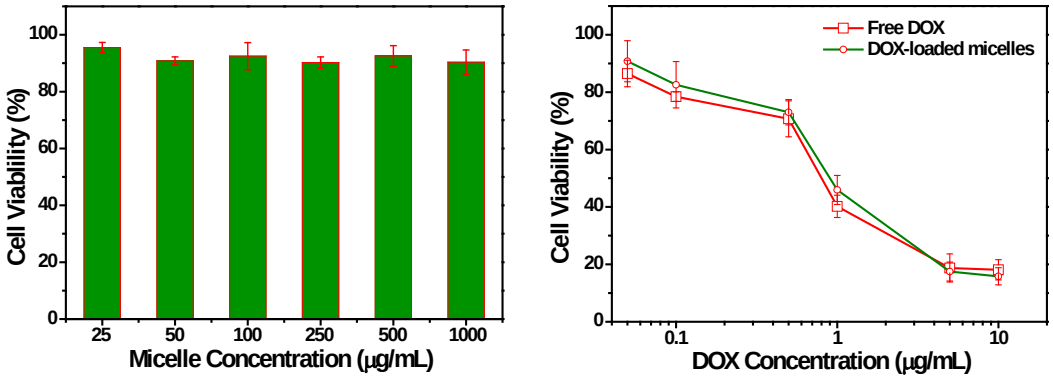

Fig. 7. (a) Cell viability of HepG2 cells following 24 h incubation with various concentrations of SC20 micelles; (b) Cell viability of HepG2 cells following 24 h incubation with free DOX and DOX-loaded SC20 micelles as a function of DOX dosages. The data were reported as the mean ± SD (n = 3).

4. Conclusions

Amphiphilic star copolymers with HyperMacs core containing disulfide bonds were prepared through two-step CuAAC reaction and their micelles were used as reduction-responsive carriers for triggered release of anti-cancer drug. The HyperMacs core was prepared from disulfide bond-containing AB_2 macromonomers of PCL, followed by grafting with PEG. The HyperMacs was found to reduce degree of crystallinity due to numerous branched structures. Combining its larger cavities and reduction-responsivity, the HyperMacs was ideal inner core of polymeric micelles for triggered release of anti-cancer drug. The as prepared star copolymers can self-assemble into spherical micelles in aqueous media, possessing good stability in neutral environment and reduction-cleavable property in reductive environment. Interestingly, these star copolymers exhibited excellent stability with a 10 times lower CMC value and a 5 times higher drug loading content as compared to their linear counterparts. In addition, the *in vitro* DOX release behavior showed slow drug release

in PBS and rapid release in a reductive environment. The cellular uptake and cytotoxicity tests showed that DOX-loaded micelles possessed a reduction-triggered release manner, good biocompatibility, and comparable anticancer activity. It is envisioned that the reduction-responsive micelles from as prepared star copolymers can be used for triggered release of anticancer drug to improve chemotherapy of cancer.

Acknowledgements

The financial support from National Natural Science Foundation of China (21374089/ 21604065) is acknowledged. J.K. thanks the grant from the Shaanxi Natural Science Funds for Distinguished Young Scholars. The financial support provided by China Scholarship Council (CSC, grant no. 201706290175) is also greatly acknowledged.

Appendix A. Supplementary material

Supplementary data associated with this article can be found, in the online version, at http://dx.doi.org/10.1016/j.eurpolymj.XX.

References

[1] A. Blanazs, S. P. Armes, A. J. Ryan, Self-assembled block copolymer aggregates: from micelles to vesicles and their biological applications. Macromol. Rapid Commun. 30 (2009) 267−277.

[2] Z. L. Tyrrell, Y. Shen, M. Radosz, Fabrication of micellar nanoparticles for drug delivery through the self-assembly of block copolymers. Prog. Polym. Sci. 35 (2010) 1128−1143.

[3] Q. Ban, T. Bai, X. Duan, J. Kong, Noninvasive photothermal cancer therapy nanoplatforms via integrating nanomaterials and functional polymers. Biomater. Sci. 5 (2017) 190−210.

[4] R. K. O. Reilly, C. J. Hawker, K. L. Wooley, Cross-linked block copolymer micelles: functional nanostructures of great potential and versatility. Chem. Soc.

Rev. 35 (2006) 1068−1083.

[5] Y. Li, K. Xiao, J. Luo, W. Xiao, J. S. Lee, A. M. Gonik, J. Kato, T. A. Dong, K. S. Lam, Well-defined, reversible disulfide cross-linked micelles for on-demand paclitaxel delivery. Biomaterials 32 (2011) 6633−6645.

[6] Q. Yin, J. Shen, Z. Zhang, H. Yu, Y. Li, Reversal of multidrug resistance by stimuli-responsive drug delivery systems for therapy of tumor. Adv. Drug Delivery Rev. 65 (2013) 1699−1715.

[7] X. Zhang, H. Dong, S. Fu, Z. Zhong, R. Zhuo, Redox‐responsive micelles with cores crosslinked via click chemistry. Macromol. Rapid Commun. 37 (2016) 993−997.

[8] H. Cho, J. Gao, G. S. Kwon, PEG-b-PLA micelles and PLGA-b-PEG-b-PLGA sol-gels for drug delivery. J. Control. Release 240 (2016) 191−201.

[9] Q. Wang, J. Jiang, W. Chen, H. Jiang, Z. Zhang, X. Sun, Targeted delivery of low-dose dexamethasone using PCL–PEG micelles for effective treatment of rheumatoid arthritis. J. Control. Release 230 (2016) 64−72.

[10] X. Cao, Z. Li, X. Song, X. Cui, P. Cao, H. Liu, F. Cheng, Y. Chen, Core-shell type multiarm star poly(ε-caprolactone) with high molecular weight hyperbranched polyethylenimine as core: Synthesis, characterization and encapsulation properties. Eur. Polym. J. 44 (2008) 1060−1070.

[11] X. Xue, J. Yang, W. Huang, H. Yang, B. Jiang, Synthesis of hyperbranched poly(ε-caprolactone) containing terminal azobenzene structure via combined ring-opening polymerization and “click” chemistry. Polymers 7 (2015) 1248−1268.

[12] S. Corneillie, M. Smet, PLA architectures: the role of branching. Polym. Chem. 6 (2015) 850−867.

[13] X. Xiong, A. Falamarzian, S. M. Garg, A. Lavasanifar, Engineering of amphiphilic block copolymers for polymeric micellar drug and gene delivery. J.

Control. Release 155 (2011) 248−261.

[14] X. Shuai, H. Ai, N. Nasongkla, S. Kim, J. Gao, Micellar carriers based on block copolymers of poly(ε-caprolactone) and poly(ethylene glycol) for doxorubicin delivery. J. Control. Release 98 (2004) 415−426.

[15] E. A. Rainbolt, K. E. Washington, M. C. Biewer, M. C. Stefan, Recent developments in micellar drug carriers featuring substituted poly(ε-caprolactone)s. Polym. Chem. 6 (2015) 2369−2381.

[16] D. Wang, T. Zhao, X. Zhu, D. Yan, W. Wang, Bioapplications of hyperbranched polymers. Chem. Soc. Rev. 44 (2015) 4023−4071.

[17] S. Wang, X. Fan, J. Kong, A new controllable approach to synthesize hyperbranched poly(siloxysilanes). J. Polym. Sci., part A: Polym. Chem. 46 (2008) 2708−2720.

[18] S. Wang, X. Fan, J. Kong, Y. Liu, Synthesis, characterization, and UV curing kinetics of hyperbranched polycarbosilane. J. Appl. Polym. Sci. 107 (2008) 3812−3822.

[19] Q. Zhang, J. Ye, Y. Lu, T. Nie, D. Xie, Q. Song, H. Chen, G. Zhang, Y. Tang, C. Wu, Z. Xie, Synthesis, folding, and association of long multiblock $(PEO_{23}\text{-b-}PNIPAM_{124})_{750}$ chains in aqueous solutions. Macromolecules 41 (2008) 2228−2234.

[20] H. Chen, J. Kong, Hyperbranched polymers from A_2+B_3 strategy: recent advances in description and control of fine topology. Polym. Chem. 7 (2016) 3643−3663.

[21] D. Yang, J. Kong, 100% hyperbranched polymers via the acid-catalyzed Friedel-Crafts aromatic substitution reaction. Polym. Chem. 7 (2016) 5226−5232.

[22] M. Trollsas, B. Atthoff, H. Claesson, J. K. Hedrick, Hyperbranched Poly(ε-caprolactone)s. Macromolecules 31 (1998) 3439−3445.

[23] J. Choi, S. Y. Kwak, Synthesis and characterization of hyperbranched poly(ε-caprolactone)s having different lengths of homologous backbone segments. Macromolecules 36 (2003) 8630−8637.

[24] W. Liu, C. M. Dong, Versatile strategy for the synthesis of hyperbranched poly(ε-caprolactone)s and polypseudorotaxanes thereof. Macromolecules 43 (2010) 8447−8455.

[25] L. R. Hutchings, J. M. Dodds, S. J. R. Bleming, HyperMacs: Highly branched polymers prepared by the polycondensation of AB2 macromonomers, synthesis and characterization. Macromolecules 38 (2005) 5970−5980.

[26] L. R. Hutchings, J. M. Dodds, D. Rees, S. M. Kimani, J. J. Wu, E. Smith, HyperMacs to HyperBlocks: A novel class of branched thermoplastic elastomer. Macromolecules 42 (2009) 8675−8687.

[27] L. Li, C. He, W. He, C. Wu, Formation kinetics and scaling of “defect-free” hyperbranched polystyrene chains with uniform subchains prepared from seesaw-type macromonomers. Macromolecules 44 (2011) 8195−8206.

[28] M. Jikei, M. Suzuki, K. Itoh, K. Matsumoto, Y. Saito, S. Kawaguchi, Synthesis of hyperbranched poly(l-lactide)s by self-polycondensation of AB_2 macromonomers and their structural characterization by light scattering measurements. Macromolecules 45 (2012) 8237−8244.

[29] M. Jikei, D. Uchida, K. Matsumoto, R. Komuro, M. Sugimoto, Synthesis and properties of long-chain branched poly(ether sulfone)s by self-polycondensation of AB_2 type macromonomers, J. Polym. Sci., Part A: Polym. Chem. 52 (2014) 1825−1831.

[30] L. R. Hutchings, S. Agostini, I. W. Hamley, D. Hermida-Merino, Chain architecture as an orthogonal parameter to influence block copolymer morphology. Synthesis and characterization of hyperbranched block copolymers: HyperBlocks. Macromolecules 48 (2015) 8806−8822.

[31] J. Li, Y. Xiang, S. Zheng, Hyperbranched block copolymer from AB_2 macromonomer: Synthesis and its reaction-induced microphase separation in epoxy thermosets, J. Polym. Sci., Part A: Polym. Chem. 54 (2016) 368−380.

[32] L. R. Hutchings, DendriMacs and HyperMacs – emerging as more than just model branched polymers, Soft Matter 4 (2008) 2150−2159.

[33] Q. Ban, J. Kong, Intramolecular cyclization of long-chain hyperbranched polymers (HyperMacs) from A_2+B_n step-wise polymerization. Polym. Chem. 7 (2016) 4717−4727.

[34] Y. Yuan, A. Zhang, J. Ling, L. Yin, Y. Chen, G. Fu, Well-defined biodegradable amphiphilic conetworks. Soft Matter 9 (2013) 6309−6318.

[35] J. Han, D. Zhu, C. Gao, Fast bulk click polymerization approach to linear and hyperbranched alternating multiblock copolymers. Polym. Chem. 4 (2013) 542−549.

[30] Y. P. Li, K. Xiao, W. Zhu, W. B. Deng, K. S. Lam, Stimuli-responsive cross-linked micelles for on-demand drug delivery against cancers. Adv. Drug Delivery Rev. 66 (2014) 58−73.

[31] A. S. Hoffman, Stimuli-responsive polymers: Biomedical applications and challenges for clinical translation. Adv. Drug Delivery Rev. 65 (2013) 10−16.

[32] S. Zhang, J. Xu, H. Chen, Z. Song, Y. Wu, X. Dai, J. Kong, Acid-leavable unimolecular micelles from amphiphilic star copolymers for triggered release of anticancer drugs. Macromol. Biosci. 17 (2017) 1600258.

[33] A. Klaikherd, C. Nagamani, S. Thayumanavan, Multi-stimuli sensitive amphiphilic block copolymer assemblies. J. Am. Chem. Soc. 131 (2009) 4830−4828.

[34] M. E. Caldorera-Moore, W. B. Liechty, N. A.Peppas, Responsive theranostic systems: Integration of diagnostic imaging agents and responsive controlled release drug delivery carriers. Acc. Chem. Res. 44 (2011) 1061−1070.

[35] M. Huo, J. Yuan, L. Tao, Y. Wei, Redox-responsive polymers for drug delivery: from molecular design to applications. Polym. Chem. 5 (2014) 1519−1528.

[36] X. Duan, T. Bai, J. Du, J. Kong, One-pot synthesis of glutathione-responsive amphiphilic drug self-delivery micelles of doxorubicin-disulfide-methoxy polyethylene glycol for tumor therapy. J. Mater. Chem. B 6 (2018) 39−43.

[37] T. Bai, J. Du, J. Chen, X. Duan, H. Chen, J. Kong, Reduction-responsive dithiomaleimide-based polymeric micelles for controlled anti-cancer drug delivery and bioimaging. Polym. Chem. 8 (2017) 7160−7168.

[38] A. Russo, W. DeGraff, N. Friedman, J. B. Mitchell, Selective modulation of glutathione levels in human normal versus tumor cells and subsequent differential response to chemotherapy drugs. Cancer Res. 46 (1986) 2845−2848.

[39] J. Y. Liu, Y. Pang, W. Huang, Z. Y. Zhu, Y. F. Zhou, D. Y. Yan, Redox-responsive polyphosphate nanosized assemblies: A smart drug delivery platform for cancer therapy. Biomacromolecules 12 (2011) 2407−2415.

[40] M. H. Lee, Z. G. Yang, C. W. Lim, Y. H. Lee, S. D. Bang, C. Kang, J. S. Kim, Disulfide-cleavage-triggered chemosensors and their biological applications. Chem. Rev. 113 (2013) 5071−5109.

[41] S. Zhang, H. Chen, J. Kong, Disulfide bonds-containing amphiphilic conetworks with tunable reductive-cleavage. RSC Adv. 6 (2016) 36568−36575.

[42] X. Duan, H. Chen, L. Fan, J. Kong, Drug self-assembled delivery system with dual responsiveness for cancer chemotherapy. ACS Biomater. Sci. Eng. 2 (2016) 2347−2354.

[43] K. Liang, G. K. Such, Z. Zhu, S. J. Dodds, A. P. Johnston, J. Cui, Engineering cellular degradation of multilayered capsules through controlled cross-linking. ACS Nano 6 (2012) 10186−10194.

[44] S. Y. An, S. M. Noh, J. H. Nam, J. K. Oh, Dual sulfide-disulfide crosslinked networks with rapid and room temperature self-healability. Macromol. Rapid

Commun. 36 (2015) 1255−1260.

[45] J. Lee, M. N. Silberstein, A. A. Abdeen, S. Y. Kim, K. A. Kilian, Mechanochemical functionalization of disulfide linked hydrogels. Mater. Horiz. 3 (2016) 447−451.

[46] F. Zhao, H. Yin, J. Li, Supramolecular self-assembly forming a multifunctional synergistic system for targeted co-delivery of gene and drug. Biomaterials 35 (2014) 1050−1062.

[47] V. Crescenzi, G. Manzini, G. Calzolari, C. Borri, Thermodynamics of fusion of poly-β-propiolactone and poly-ϵ-caprolactone. Comparative analysis of the melting of aliphatic polylactone and polyester chains. Eur. Polym. J. 8 (1972) 449−463.

[48] M. Möller, R. Kånge, J. L. Hedrick, $Sn(OTf)_2$ and $Sc(OTf)_3$: Efficient and versatile catalysts for the controlled polymerization of lactones, J. Polym. Sci., Part A: Polym. Chem. 38 (2000) 2067−2074.

[49] H. R. Kricheldorf, A. Stricker, D. Langanke, Polylactones, 50. The reactivity of cyclic and noncyclic dibutyltin bisalkoxides as initiators in the polymerization of lactones, Macromol. Chem. Phys. 202 (2001) 2525–2534.

[50] J. Ling, J. Liu, Z. Shen, T. E. Hogen-Esch, Ring-opening polymerization of ε-caprolactone catalyzed by Yttrium trisphenolate in the presence of 1,2-propanediol. Do both primary and secondary hydroxyl groups initiate polymerization? J. Polym. Sci., Part A: Polym. Chem. 49 (2011) 2081−2089.

[51] M. Prabaharan, J. J. Grailer, S. Pilla, D. A. Steeber, S. Gong, Folate-conjugated amphiphilic hyperbranched block copolymers based on Boltorn® H40, poly(l-lactide) and poly(ethylene glycol) for tumor-targeted drug delivery. Biomaterials 30 (2009) 3009−3019.

[52] P. Zhou, Y. Y. Liu, L. Y. Niu, J. Zhu, Self-assemblies of the six-armed star triblock ABC copolymer: pH-tunable morphologies and drug release. Polym.

Chem. 6 (2015) 2934−2944.

[53] H. Chen, J. Jia, X. Duan, Z. Yang, J. Kong, Reduction-cleavable hyperbranched polymers with limited intramolecular cyclization via click chemistry. J. Polym. Sci., Part A: Polym. Chem. 53 (2015) 2374−2380.

[54] J. Y. Liu, Y. Pang, W. Huang, Z. Y. Zhu, X. Y. Zhu, Y. F. Zhou, D. Y. Yan, Redox-responsive polyphosphate nanosized assemblies: A smart drug delivery platform for cancer therapy. Biomacromolecules 12 (2011) 2407−2415.